American Mineralogist, Volume 62, pages 278–285, 1977

Characterization of a marine birnessite

E. D. GLOVER

Department of Geology and Geophysics
University of Wisconsin, Madison, Wisconsin

Abstract

Birnessite, more crystalline than has been heretofore described, has been found in micronodules from a depth of 2–4 meters below the top of a Caribbean core in foraminiferal sediments. The associated sediments have been carbon-dated at 33,640 ± 5340 years.

The mineral has been studied by scanning electron microscopy, X-ray diffraction, and electron microprobe analysis. The surface structure is made up of curved, intersecting plates between 500–1000 A thick. The X-ray data agree reasonably well with the data on synthetic birnessite compounds. The chemical formula, by analogy with chalcophanite, is $(Na, Ca, K)_{0.83}Mg_{1.04}Mn_{5.96}(Fe, Co, Ni, Cu)_{0.16}O_{13.6}(H_2O)_{3.8}$. The assignment of this formula with Mn in the + 4 valence state leans heavily on the findings for the synthetic compounds since no analysis was made for the Mn valence state(s) or the amount of water present.

Introduction and general description

Birnessite and todorokite are two of the most important manganese minerals comprising ferromanganese nodules. Their content of first transition-group metals in certain regions of the sea floor, often at economically important levels, has led to mushrooming research on nodule genesis. Because the manganese oxide phases are typically intermixed on a fine scale with iron oxides (Burns and Burns, 1976), as well as with other authigenic and detrital minerals, they are difficult to characterize.

I have found an occurrence of these two minerals where one of them (birnessite) occurs with a more ordered crystal structure than has hitherto been reported for the mineral. The material is in a core from the Gulf of Mexico just south of the northwest tip of Cuba in 2244 meters of water in hemipelagic, foraminiferal sediments (Atlantis cruise A–185–23, May 15, 1953; Lat. 21°32′N, Long. 85°4.5′W, Ewing *et al.*, 1958). The zone of occurrence of manganese minerals is from 200–400 cm below the top of the core. The sediments have been carbon-dated at the 240–245 cm level, giving an apparent age of 33,640 ± 5,340 years (H. F. Nelson, personal communication).

The manganese oxides are found in microclusters, usually on or in foraminifer tests. The most abundant occurrence is in a zone at the 240 cm level, where they may be noticed with the naked eye as a scattered, black discoloration of the calcium carbonate skeletal material. The clusters at this level contain mainly birnessite and todorokite, as indicated by X-ray diffraction, both minerals occurring in the same cluster. At the 300 cm level and below, the clusters are almost exclusively birnessite. They are a few tenths of a millimeter or less in diameter. To date a number of birnessite clusters have been collected and studied, but no clusters are exclusively todorokite. Photomicrography, study of the X-ray diffraction effects, and chemical analysis of the birnessite clusters have been carried out in order to characterize this marine birnessite as to structure and composition.

Observations with the scanning electron microscope (SEM)

Birnessite was originally described by Jones and Milne (1956) as composed of black grains. More recently scanning electron microscope examination has shown a profusion of surface structures on a scale of a few microns or less: plates, disks, box-work of intersecting plates or disks, box-work of curved plates with crenulate edges (Woo, 1973); sponge-work, aggregates or botryoidal clusters of spherulites (Fewkes, 1973; Sorem and Fewkes, 1976); and clusters with a cellular structure of bent plates (Brown *et al.*, 1971).

The present material shows many of these same features, but the most characteristic surface structure is that of intergrown curved plates or surfaces which, seen end-on, appear vermiform. Figure 1 shows SEM photos of birnessite clusters Nos. 1 and 2 at two different magnifications. In the original photographs, at the highest magnification (30,000 ×), one can see a banding or lineation on the termination of the individual curved plates of cluster No. 1. This seems to indicate substructure smaller than the 600–1200A thickness of the platelets. However, the revelation of this apparent substructure may be the result of evacuation in the SEM or the heat of the carbon arc in vacuo while carbon coating.

X-ray diffraction results

To observe the X-ray diffraction effects, the cluster to be examined was glued to a freshly-made glass fiber, placed in a 57.3 mm or 114.6 mm diameter powder camera, and rotated in unfiltered or filtered Fe radiation. Because of their roughly spherical growth, the clusters gave excellent powder patterns, even without rotation. The birnessite clusters also contain small amounts of calcite (foram shell particles, coccoliths, possible secondary calcite), quartz, and euhedral zeolite crystals, probably phillipsite. The accessory mineral lines were usually easily distinguished from the birnessite lines on the basis of their spotty character or greater sharpness.

In Table 1 X-ray diffraction patterns of clusters 1 and 2 are compared with published data. The reference patterns are from (synthetic) manganese (III) manganate (IV) (Giovanoli *et al*., 1970b) (Cols. 5, 6, and 7), which is presently accepted as being equivalent to birnessite by the Powder Diffraction File editors (for a complete critical discussion of X-ray data see Burns and Burns, 1976). The reflections found

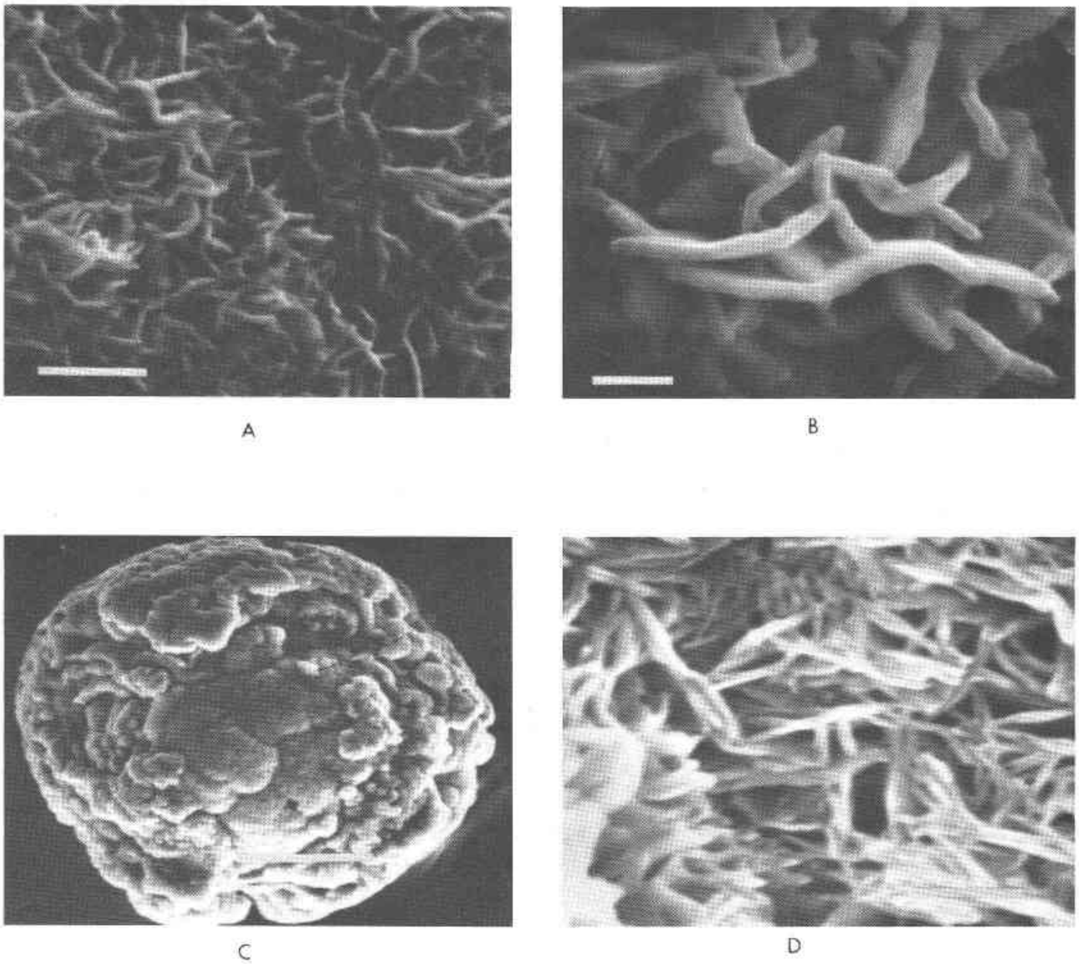

FIG. 1. SEM pictures of birnessite clusters No. 1 and 2. Surface of No. 1, (a) and (b); surface of No. 2, (c) and (d). Length of bar in microns: (a) 2, (b) 0.5, (c) 50, (d) 1.

TABLE 1. X-ray diffraction data from birnessite

Birnessite, This Study				Manganese Oxide Hydrate, Giovanoli et al. - Powder Diffraction File Card 23-1239		
Cluster No. 1*		Cluster No. 2**				
(1) d-spacing	(2) I/Io†††	(3) Meas. d-spacing	(4) Calc. d-spacing	(5) d-spacing	(6) I/Io	(7) hkl
7.08	100	7.06	7.11	7.21	100	001
3.547	28	3.556	(3.556)†	3.61	80	002
2.468	17	2.464	2.467	2.46	100	100
2.333	43	2.330	2.330	2.33	100	101
2.031	24	2.027	2.027	2.04	80	102
1.775	1	1.775	1.778	1.802	10	004
1.711	29	1.710	1.709	1.723	80	103
	1	1.447	1.442	1.454	20	104
1.426	17	1.424	(1.424)††	1.422	60	110
1.398	10	1.397	1.396	1.391	40	111
	4	1.322	1.322	1.321	20	112
1.234	6	1.231	1.233	1.229	20	200
1.219	6	1.215	1.215	1.212	20	201
1.185	4	1.182	1.185			006
1.167	4	1.163_5	1.165_1	1.164	10	202
1.105	5	1.093_6	1.094_0	1.094	10	203
	5	1.014_2	1.013_3	1.015	10	204
				0.929	10	210
				0.905	10	008
				0.867	10	213
				0.819	10	300

* Unfiltered Fe radiation, 114.6 mm camera, not corrected for shrinkage. Three Kβ lines from birnessite plus 3 (Kα) lines from calcite omitted.

** Filtered Fe radiation, 57.3 mm camera, corrected for shrinkage. Barely perceptible main calcite reflection omitted.

† Used to estimate c.

†† Used to estimate a.

††† Estimates of intensities of lines with $I/I_o \geq 10$ were made by visual comparison of lines with a timed exposure series of spots under a low-power microscope. These values were multiplied by estimates of line widths made by direct measurement to give the reported intensity values. The remaining weak lines were estimated visually. Thus, the measurement of the strong lines gives numbers approximating integrated intensities.

agree with those of Giovanoli *et al.*, with the limitation that Fe radiation was used (not molybdenum), except that the (006) reflection was present. It was quite easily distinguished from the nearby (202) reflection and measured, even with a film made in the small camera. In fact, the relatively good line resolution in patterns from the natural material would seem to make the present specimen the best crystallized example of the birnessite structure yet found, synthetic or natural.

The *d* values agree fairly well with the Giovanoli *et al.* data, the most obvious difference being a lower value of *c* in the subject specimen. The intensities, however, differ markedly. This is not surprising, since the composition of the natural mineral differs from the synthetic reference compound (see below). In films made with Fe radiation, where there is sufficient resolution of the diffraction pattern, one can see with the naked eye that (*hk*0) and (00*l*) reflections are relatively sharp, while (*hkl*) reflections are noticeably broadened. The interpretation here is that there is reasonably good order within the layers of the proposed structure (Giovanoli *et al.*, 1970b) and a relatively uniform stacking sequence of ~7A layers.

There is, however, much less order in the registration of the adjacent layers, and the situation is quite comparable, as Giovanoli *et al.* (1970a,b) have noted, to the layer structure of some of the 7A clay minerals.

Chemical analysis

Qualitative analysis was carried out in both the SEM and the electron probe. Present in the birnessite are: Mn (main constituent); Na, Mg, K, and Ca, each in sizeable amounts (0–7% level); Fe, Co, Cu, and Ni, each < 1 percent, with usually $Ni > Fe > Cu > Co$. Thus the present material shows the characteristic of manganese nodule minerals of 'scavenging' transition metals. Other elements revealed by their X-ray spectra are Cl, S, and Si. They occur in small and variable amounts and are thought to be adventitious.

A complete quantitative analysis of these small specimens is limited by the fact that neither the percentage of Mn reduced below valence 4, the oxygen content, nor the water content can very easily be determined. Also, the vacuum used in microbeam analysis may cause loss of some of the water of crystallization before the analysis can be made. Nevertheless, valuable information may be obtained, especially using the low beam current of a SEM equipped with the highly sensitive EDS system (energy dispersive spectrometer). In this way a complete analysis may usually be carried out for elements above fluorine, where concentrations are above a few tenths of a percent, with beams of very small radius with high spatial resolution. Point by point concentrations of all major and minor elements above fluorine are obtained. This has been done on the two clusters of birnessite seen in Figure 1 which were used previously for X-ray diffraction, the transition elements being analyzed by the wavelength dispersive system (WDS) of the probe. An example of the results[1] for one sample point of cluster No. 2 (point No. 1) are given in Table 2.

Discussion

Formula of birnessite

If the data are cast into the formula corresponding to the structure proposed by Giovanoli *et al* .,1970b (assuming 7 Mn atoms) then the oxygen content is high (20.8 calculated by difference *vs.* 18 for the reference formula). If one assumes 7 (Mg + Mn) then the average formula is:

$$Na_{0.46}\ Ca_{0.12}\ K_{0.25}\ Mg_{1.04}\ Mn_{5.96}\ (Fe_{0.05}\ Co_{0.02}\ Ni_{0.07}\ Cu_{0.03})\ O_{13.6}\ (H_2O)_{3.8}.$$

Written more compactly the formula may be compared to the two previously proposed formulae for birnessite (Jones and Milne, 1956; Brown *et al.* 1976), the two proposed forms of Giovanoli *et al.*, and the proposed (Giovanoli *et al.* 1970a,b) related structure, chalcophanite (Wadsley, 1955):

This study
$(Na, Ca, K)_{0.83}\ Mg_{1.04}\ Mn_{5.96}\ (Fe, Co, Ni, Cu)_{0.16}\ O_{13.6}\ (H_2O)_{3.8}$
Jones and Milne
$(Na_{0.7}\ Ca_{0.3})\ Mn_7O_{14}\ (H_2O)_{2.8}$
Brown et al.
$(Na_{0.54}\ Ca_{0.51})\ (Mn^{2+}_{0.65},\ Mn^{4+}_{6.34})\ O_{14.1}\ (H_2O)_{2.9}$
Manganese oxide hydrate, Powder Diffraction File Card 23-1239
$(Mn^{3+}_2,\ Mn^{4+}_5)\ O_{13.0}\ (H_2O)_{4.95}$
Sodium manganese oxide hydrate, Powder Diffraction File Card 23-1046
$Na_2\ (Mn^{3+}_{1.0}\ Mn^{2+}_{1.0}\ Mn^{4+}_5)\ O_{13.5}\ (H_2O)_{4.5}$
Chalcophanite
$Zn_2\ (Mn^{4+}_6)\ O_{14}\ (H_2O)_6.$

This comparison shows the apparent occurrence of Mg in place of some of the lower-valence Mn of the maganese oxide hydrate. It shows a Na + K + Ca content of 0.83 atoms, which is intermediate between the two reference compounds of Giovanoli *et al.* It shows a total of about 0.16 atoms of transition metals, which are not present in the synthetic compounds but are present in the related marine mineral; and it

TABLE 2. Analysis at one sample point of cluster No. 2

Na_2O	MgO	SiO_2	Cl	S	K_2O	CaO	MnO_2	FeO	CoO	NiO	CuO	Total
1.9*	6.2	0.9	0.1	0.2	1.8	0.39	75.8	0.55	0.14	0.80	0.33	88.9

* All numbers in weight percent.

---

[1] For complete data and a discussion of the analysis see Appendix.

indicates a variable water content, which may be expected when analyzing hydrates in a vacuum. (All probe work is consistent with this loss. Whereas the ratio of other elements to Mn is fairly consistent—some elements, such as K and Mg, more than others—the ratio of Mn to oxygen [by difference] varies considerably with the analytical conditions during analysis of the sample: beam voltage, current, and area of specimen sampled by the beam). Thus this composition agrees well with the Giovanoli *et al.* compounds but has a very similar formula overall to those of Jones and Milne and of Brown *et al.*; the striking difference is the high Mg and K content, which is consistent with the marine origin and possibly may be characteristic of it.

The ideal structure of chalcophanite (Wadsley, 1955), to which Giovanoli *et al.* (1970a,b) believe birnessite is related, is a layer structure composed of a $Mn_4{}^+$–O octahedral sheet alternating with a sheet composed of Zn atoms coordinated to oxygen and water. In most examples of chalcophanite part of the Mn is present as Mn^{2+} (Wadsley, 1955). The proposed formula (basis, Mn + Mg = 7) of the present sample is equivalent to scaling the numbers of atoms present on the basis of 6 Mn^{4+} (see analysis results, Tables 3, 4 and 5 in the Appendix). This could be written: $(Na, Ca, K, Fe, Co, Ni, Cu)_{0.99}\,Mg_{1.04}\,Mn_6\,O_{\sim 14}\,(H_2O)$ where Mg and the sum of Na, Ca, K, Fe, Co, Cu, and Ni formally correspond to the two Zn atoms of chalcophanite.

With synthetic birnessites Feitknecht and Marti, and Buser *et al.* (reviewed in Burns and Burns, 1976) found that the higher the oxidation state of Mn the poorer was the stacking of the layers, giving a diffuse or absent 7A spacing. Also, structural arguments (Burns and Burns, 1976) that Mn^{2+} substituting for Mn^{4+} in the octahedral Mn–O sheet gives necessary stability would seem to associate the higher oxidation state with poor crystallinity. For these reasons and because most chalcophanites themselves contain some Mn^{2+}, Mn is probably present in this relatively well-crystallized specimen partly as Mn^{2+}, in either the Mn–O octahedral sheet, the alternating sheet, or both.

The fitting of the data to the above formula could not have been accomplished with any assurance without the basic data of Giovanoli *et al.*, because a complete chemical analysis could not be done. If one accepts their estimate of the probable structure, then the comparison of the present sample to their manganese oxide hydrate is recapitulated as follows: The present sample gives an X-ray diffraction pattern agreeing reasonably well with the pattern of the hexagonal synthetic compound within the limitation of the range of *d* spacings covered by the Fe radiation used, with one additional basal order (006) visible in the pattern of the present sample. If one casts the chemical analysis into their form, one obtains a formula intermediate between their two compounds, with other ions (K, Ca, Mg) replacing some of the

TABLE 3. Number of atoms in formula for cluster No. 1*

Na	K	Ca	ΣK NaCa	ΣNaCa	Si	Mg	Mn	ΣMgMn	ΣKNaCa +T.M.**	Cl	O	H_2O
0.49	0.25	0.06	0.80	0.73	0.04	1.01	6.00	7.01	0.96	0.18	13.5	1.5
0.29	0.24	0.15	0.68	0.71	0.05	1.00	6.00	7.00	0.84	0.27	13.5	1.0
0.58	0.26	0.06	0.90	0.75	0.02	1.05	6.00	7.05	1.06	0.11	13.6	1.1
0.47	0.24	0.11	0.82	0.69	0.00	1.01	6.00	7.01	0.98	0.11	13.5	1.1
0.39	0.25	0.15	0.79	0.68	0.03	1.07	6.00	7.07	0.95	0.14	13.6	3.5
0.40	0.26	0.11	0.77	0.63	0.05	1.16	6.00	7.16	0.93	0.13	13.6	3.3
0.45	0.27	0.26	0.98	0.87	0.15	1.10	6.00	7.10	1.14	0.17	13.7	3.7
0.46	0.27	0.23	0.96	0.83	0.05	1.06	6.00	7.06	1.12	0.14	13.7	1.7
0.21	0.24	0.36	0.81	0.74	0.15	1.05	6.00	7.05	0.97	0.17	13.7	5.8
0.23	0.25	0.23	0.71	0.60	0.15	1.02	6.00	7.02	0.87	0.14	13.5	4.4
0.28	0.27	0.10	0.65	0.51	0.07	0.99	6.00	6.99	0.81	0.13	13.4	3.0

* Each line in body of table represents analysis at one sample point. Analysis of transition elements by WDS system of electron microprobe, all other analyzed elements by EDS system of SEM, O and H_2O by difference.

** Transition Metals: average of 3 points on cluster No. 1.
Fe 0.050(3), Co 0.010(1), Ni 0.070(4), Cu 0.030(3)
Σ Fe, Co, Ni, Cu = T.M. = 1.60(6)

TABLE 4. Number of atoms in formula for cluster No. 2*

Na	K	Ca	ΣKNaCa	ΣNaCa	Si	Mg	Mn	ΣMgMn	ΣKNaCa +T.M.**	Cl	S	O	H_2O	$O+H_2O$
0.43	0.27	0.05	0.75	0.48	0.1	1.06	6.00	7.06	0.91	0.02	0.03	13.6	4.2	17.7
0.64	0.24	0.07	0.95	0.71	0.02	0.99	6.00	6.99	1.11	0.02	0.06	13.7	3.7	17.4
0.45	0.24	0.06	0.75	0.51	0.3	1.06	6.00	7.06	0.91	0.0	0.0	13.4	5.8	19.2
0.55	0.23	0.06	0.84	0.61	0.2	1.10	6.00	7.10	1.00	0.0	0.02	13.3	5.6	18.9
0.57	0.26	0.07	0.90	0.64	0.07	1.00	6.00	7.00	1.06	0.0	0.04	13.5	6.4	18.9

* Each line in body of table represents analysis at one sample point. Analysis of transition elements by WDS system of electron microprobe, all other analyzed elements by EDS system of SEM, O and H_2O by difference.

** Transition Metals: average of 3 points on cluster No. 1
Fe 0.050(3), Co 0.010(1), Ni 0.070(4), Cu 0.030(3)
Σ Fe, Co, Ni, Cu = T.M.= 0.160(6)

sodium and manganese of the postulated interlayer, a formula agreeing well, overall, with previous proposals for birnessite and with chalcophanite.

Significance of Mg and K

The presence of high Mg and moderate K concentrations, showing little variability with respect to Mn, strongly suggests consideration of this compositional relationship as a possible characteristic of marine birnessite. In fact, this observation agrees well with the correlation made by Burns and Furstenau (1966), using X-ray maps of K, Mg, and Mn in a marine 7A Mn–O mineral phase, presumably a birnessite-like form. Other analyses of ferromanganese nodule material have not shown this correlation, either because (1) Mg and K were not measured, or (2) the Mg or K level was more or less uniform and/or not strongly associated with any one phase, or (3) no identification was made of the mineral species being analyzed.

In the study of Burns and Furstenau (1966) Mn–O phases thought to be a more disordered 'δ Mn O_2' species (Burns and Burns, 1976) did not show the K, Mg, Mn correlation.

Since it has not been possible as yet to separate the supposed todorokite phase (9.6A) in the present material, it is not known with any certainty whether or not this todorokite contains K and Mg. Other analyses have not revealed a Mg, K, Mn association for marine todorokites.

It is hoped that techniques similar to those described here, plus electron diffraction studies applied to the present material and other nodule material, may clarify further the Mg, K, Mn association.

Summary

(1) The birnessite described here differs from previously described materials in several respects. (a) Its content of Na, Mg, K, and Ca is different from that of any previously documented specimens, but its bulk formula is analogous with previously described birnessites and resembles closely the chalcophanite formula on which its structure may be based. (b) It is better ordered, structurally, than any previously described birnessite mineral. (c) It is the first natural birnessite in which the X-ray diffraction pattern agrees with the presently accepted diffraction data for the synthetic analog in all important details, and with a proposed formulae bracketed by the synthetic (birnessite) and Na (birnessite) forms.

(2) The finding and characterization of this mineral lends support to the proposal that the hexagonal structure of manganese oxide hydrate of Giovanoli *et al.* (Powder Diffraction File Card 23-1239) is a valid reference for the naturally occurring birnessite minerals.

(3) The K and Mg content suggests a possibly important marine association and demands consideration of the role of K and Mg in ferromanganese nodule genesis.

Appendix

Chemical analysis

After SEM photography and X-ray diffraction the approximately 0.1 mm diameter grains were flattened on the glyptal-smeared surface of a 1" epoxy plug and vacuum-coated with carbon. Since the major contaminant was $CaCO_3$ (from the admixed coccol-

TABLE 5. Final hypothesized formulae for each sample point of clusters Nos. 1 and 2: Basis, Mn^{4+} = 6 (Si, Cl and equivalent Na, and S deleted)

	Na	Ca	K	Mg	Mn	Fe	Co	Ni	Cu	O	H_2O
Cluster No. 1	0.49	0.06	0.25	1.01	6.00	0.05	0.01	0.07	0.03	13.5	1.5
	0.29	0.14	0.24	1.00	6.00	0.05	0.01	0.07	0.03	13.5	1.0
	0.58	0.06	0.26	1.05	6.00	0.05	0.01	0.07	0.03	13.6	1.1
	0.47	0.11	0.24	1.01	6.00	0.05	0.01	0.07	0.03	13.5	1.1
	0.39	0.15	0.25	1.07	6.00	0.05	0.01	0.07	0.03	13.6	3.5
	0.40	0.12	0.26	1.16	6.00	0.05	0.01	0.07	0.03	13.6	3.3
	0.45	0.26	0.27	1.10	6.00	0.05	0.01	0.07	0.03	13.7	3.7
	0.46	0.23	0.27	1.06	6.00	0.05	0.01	0.07	0.03	13.7	1.7
	0.21	0.37	0.24	1.05	6.00	0.05	0.01	0.07	0.03	13.7	5.8
	0.23	0.23	0.25	1.02	6.00	0.05	0.01	0.07	0.03	13.5	4.4
	0.28	0.10	0.27	0.99	6.00	0.05	0.01	0.07	0.03	13.4	3.0
Average	0.40(13)*	0.17(10)	0.25(1)	1.05(5)	6.00	0.05	0.01	0.07	0.03	13.6(1)	2.7(16)
Cluster No. 2	0.43	0.05	0.27	1.06	6.00	0.05	0.01	0.07	0.03	13.6	4.2
	0.64	0.07	0.24	0.99	6.00	0.05	0.01	0.07	0.03	13.7	3.7
	0.45	0.06	0.24	1.06	6.00	0.05	0.01	0.07	0.03	13.5	5.8
	0.55	0.06	0.23	1.10	6.00	0.05	0.01	0.07	0.03	13.6	5.7
	0.57	0.07	0.26	1.00	6.00	0.05	0.01	0.07	0.03	13.5	5.4
	0.53(7)	0.06(1)	0.25(1)	1.04(5)	6.00	0.05	0.01	0.07	0.03	13.6(1)	5.0(10)
Average of 2 Clusters	0.46(8)	0.12(5)	0.25(1)	1.04(5)	6.00	0.05	0.01	0.07	0.03	13.6(1)	3.8(10)

*Parenthetical figures represent the estimated standard deviation (esd), in terms of least units cited for the value to their immediate left, thus 0.40(13) indicates an esd of 0.13.

iths and, often, intergrown foraminifer chamber walls), it was necessary to select EDS analysis regions where the Ca X-ray level was at a minimum. Points accepted for analysis had a Ca peak no greater than that of K, and low or absent Si and S Peaks. The deliberate choice of sample points, then, gives results that should be qualified in that Si and S may not be negligible, and Ca values may be somewhat different than those shown (Tables 3, 4, and 5). Since the Ca values found in cluster No. 1 were variable and in some cases comparable to cluster No.2, a very low or zero value may be close to the true composition.

That part of the analysis done in the SEM was for all the elements except the transition group metals Fe, Co, Ni, and Cu. Because of the difficulties of analyzing for low concentrations in the EDS system, the analyses of the transition metals were made in the electron probe with its WDS system, where all the $K\alpha$ lines could be resolved and analyzed with greater sensitivity. Three points in cluster No. 1 were analyzed, with results and standard deviations as shown in Tables 3, 4, or 5. Typical analysis conditions for the SEM and the probe were as follows:

SEM: 15kV, 0.5–1.0 × 10^{-9} amperes, absorbed current, 50″–300″ X-ray collection time.

Standards: NaCl, KH_2PO_4, $CaCO_3$, MgO, SiO_2, Mn metal, CuS.

Electron Probe: 25kV, 6 × 10^{-8} absorbed current.

Standards: Fe, Co, Ni, Cu metals; average of sampled areas, ~20 micron diameter circle.

Correction of data

The actual routine for correction of the X-ray intensities to concentrations was as follows. Data taken at 15kV, using the EDS system, was multiple least-squares fitted by standard spectra (Schamber, 1973), then corrected using the theoretical correction program ('ZAF' corrections also by Schamber, 1974), in the PDP 11/05 computer which is part of the X-ray analysis system. Schamber's program is similar to other widely used theoretical correction programs such as J. W. Colby's "Magic 4" (1971). From the output of concentrations the numbers for Na, Mg, Si, Cl, S, Ca, K, and Mn were accepted as final as far as correction of data is concerned. Then the probe data (*K* ratios) for Fe, Co, Ni, and Cu were entered along with the known concentrations for Na, Mg, Si, Cl, S, K, Ca and Mn in the same program for correction of Fe, Co, Ni and Cu; corrections which are minimal in this case. The two correction runs were necessary since the takeoff angles are different in the two instruments. Complete analysis data for 11 points on cluster 1 and 5 points on cluster 2 are given in Tables 3 and 4. The final assessment of numbers of atoms in the formula, based on 6 Mn^{4+} atoms, is given in Table 5 for each sample point. In this tabulation Si, S, and Cl are deleted, since they are thought to be adventitious.

Methods of calculation

The method of obtaining numbers of atoms of O and H_2O was as follows: a first estimate of the O plus H_2O (or OH) content was obtained by subtracting the total of analyzed elements from 100 percent. This number was adjusted appropriately when SiO_2, and Na equivalent to Cl and SO_4 were subtracted from the analysis. This adjusted number was converted to relative number of O atoms by dividing by 16, and then multiplied by the factor necessary to give 6 atoms of Mn (or 7 atoms of Mg + Mn). This gave the total O atoms in the formula, assuming the difference of the sum of the analyzed elements from 100 percent is oxygen. When the numbers of oxygen atoms associated with the analyzed elements were added up (Mn as MnO_2), and subtracted from the total of O atoms, the remainder gave the number of water molecules on an oxygen basis. The final figure for number of water molecules was obtained, then, by multiplying by 16/18. A somewhat more accurate value might be obtained by iteration of this calculation, but this was not done, since the high variability of this number over the sample points indicates a poor accuracy for reasons already suggested (analysis in vacuum).

Acknowledgements

I wish to thank S. W. Bailey, University of Wisconsin, Madison, Wisconsin, for his advice and criticism of the X-ray data and R. G. Burns, Massachusetts Institute of Technology, Cambridge, Massachusetts, for critical comment on an early version of the manuscript. J. D. Hays and (the late) M. Ewing, Lamont-Doherty Geological Observatory, Palisades, New York, have kindly given their permission to use the A-185 cores in research on cathodoluminescence of carbonates, of which this study is a part. H. F. Nelson of Mobil Research and Development Corporation, present on the A-185 cruise, made available the cuts of the cores, which are stored at Mobil's Field Research Laboratory, Dallas, Texas, and generously supplied the C-14 date on core A-185-23.

References

Brown, F. H., A. Pabst and D. L. Sawyer (1971) Birnessite on colemanite at Boron, California. *Am. Mineral., 56,* 1057–1064.

Burns, R. G. and V. M. Burns (1976) Mineralogy of ferromanganese nodules. In G. P. Glasby, Ed., *Marine Manganese Deposits.* Elsevier Publishing Company, Amsterdam, in press.

——— and D. W. Furstenau (1966) Electron probe determination of inter-element relationships in manganese nodules. *Am. Mineral., 54,* 895–902.

Colby, J. W. (1971) MAGIC IV, A new improved version of MAGIC. *Proc. 6th Natl. Conf. Electron Probe Analysis,* Pittsburgh, Pennsylvania, July 27–30, p. 17A–17B.

Ewing, M., D. B. Ericson and B. C. Heezen (1958) Sediments and topography of the Gulf of Mexico. In L. G. Weeks, Ed., *Habitat of Oil.* AAPG, Tulsa, Oklahoma.

Fewkes, R. H. (1973) External and internal features of marine manganese nodules as seen with the SEM and their implications in nodule origin. In M. Morgenstein, Ed., *Papers on the Origin and Distribution of Manganese Nodules in the Pacific and Prospects for Exploration.* Honolulu, Hawaii, p. 21-29.

Giovanoli, R., E. Stähli and W. Feitknecht (1970a) Uber Oxidhydroxide des vierwertigen Mangans mit Schichtengitter. 1. Natrium–mangan (II, III) manganat (IV). *Helv. Chim. Acta, 53,* 209–220.

———, E. Stähli and W. Feitknecht (1970b) Uber Oxidhydroxide des vierwertigen Mangans mit Schichtengitter. 2. Mangan (III)–manganat (IV). *Helv. Chim. Acta, 53,* 453–464.

Jones, L. H. P. and A. A. Milne (1956) Birnessite, a new manganese oxide mineral from Aberdeenshire, Scotland. *Mineral. Mag., 31,* 283–288.

Schamber, F. H. (1973) A new technique for deconvolution of complex X-ray spectra. *Proc. 8th Natl. Conf. Electron Probe Analysis,* New Orleans, La., Aug. 13–17, p. 85A–85C.

——— (1974) ZAF correction procedure, Tracor Northern Techn. Lit., Tracor Northern, Inc., Middleton, Wisconsin.

Sorem, R. K. and R. H. Fewkes (1976) Internal characteristics of marine manganese nodules. In G. P. Glasby, Ed., *Marine Manganese Deposits.* Elsevier Publishing Company, Amsterdam, in press.

Wadsley, A. D. (1955) The crystal structure of chalcophanite, $ZnMn_3O_7 \cdot 3H_2O$. *Acta Crystallogr., 8,* 165–172.

Woo, C. C. (1973) Scanning electron micrographs of marine manganese micronodules, marine pebble-sized nodules, and fresh water manganese nodules. In M. Morgenstein, Ed., *Papers on the Origin and Distribution of Manganese Nodules in the Pacific and Prospects for Exploration.* Honolulu, Hawaii, p. 165–171.

Manuscript received, October 28, 1975; accepted for publication, November 2, 1976.